Published for SISSA by Springer

Received: *April 29, 2020*
Revised: *August 14, 2020*
Accepted: *September 23, 2020*
Published: *October 30, 2020*

Probing new physics scenarios of muon $g-2$ via J/ψ decay at BESIII

Gorazd Cvetič,[a] **C.S. Kim,**[b,c] **Donghun Lee**[c] **and Dibyakrupa Sahoo**[c]

[a] *Department of Physics, Universidad Tecnica, Federico Santa Maria, Valpraiso, Chile*
[b] *Institute of High Energy Physics, Dongshin University, Naju 58245, Korea*
[c] *Department of Physics and IPAP, Yonsei University, Seoul 03722, Korea*

E-mail: gorazd.cvetic@usm.cl, cskim@yonsei.ac.kr, donghun.lee@yonsei.ac.kr, sahoodibya@yonsei.ac.kr

Abstract: The disagreement between the standard model prediction and the experimental measurement of muon anomalous magnetic moment can be alleviated by invoking an additional particle which is either a vector boson (X_1) or a scalar (X_0). This new particle, with the mass $m_X \lesssim 2m_\mu$, can be searched for in the decay $J/\psi \to \mu^-\mu^+X$, where X is missing. Our numerical study shows that the search is quite feasible at the BESIII experiment in the parameter space allowed by muon $g-2$ measurements.

Keywords: Beyond Standard Model, Gauge Symmetry

ArXiv ePrint: 2004.03124

https://doi.org/10.1007/JHEP10(2020)207

JHEP10(2020)207

Contents

JHEP10(2020)207

1 Introduction

The magnetic moment of muon ($\boldsymbol{\mu}$) is directly proportional to its intrinsic spin ($\mathbf{S}$), $\boldsymbol{\mu} = g_\mu \left(\frac{e}{2m_\mu}\right) \mathbf{S}$, where g_μ, e, m_μ are the g-factor, elementary charge and mass of muon, respectively. The Dirac equation predicts $g_\mu = 2$ since muon is an elementary (i.e. structureless) spin-$\frac{1}{2}$ fermion. However, radiative corrections from quantum loops are known to result in a tiny but non-zero deviation from this value. This deviation is quantified by the anomalous magnetic moment, $a_\mu = (g_\mu - 2)/2$. The anomalous magnetic moment of muon has been very precisely measured by the E821 experiment at Brookhaven National Laboratory (BNL) [1]. The experimental measurement is found to be about 3.3σ larger than the Standard Model (SM) prediction [2],

$$\Delta a_\mu \equiv a_\mu^{\rm exp} - a_\mu^{\rm SM} = (261 \pm 63 \pm 48) \times 10^{-11}, \tag{1.1}$$

where the first error is from experiment and the second one is from theory prediction. This result, as well as the recent observation that inclusion of SM radiative corrections is not sufficient to resolve the anomaly in a_μ [3], can be considered as possible hints of some underlying new physics. Further, the contribution of the leading order hadronic vacuum polarization to the muon a_μ, extracted with high accuracy from the measurements of $e^+e^- \to$ hadrons [4, 5], also cannot reduce the present discrepancy Δa_μ. In this paper, we shall probe two simple new physics scenarios, involving either a new vector boson (say X_1) or a new scalar (say X_0), which can contribute to muon anomalous magnetic

moment and alleviate the existing discrepancy between theory prediction and experimental measurement. Our proposed search for the new particle is via the study of the decay $J/\psi \to \mu^-\mu^+ X_{0,1}$, in the range $m_X \leqslant 2m_\mu$, with $X_{0,1}$ as the invisible or missing final state. This decay mode can be studied in the ongoing BESIII experiment or in any future experiment which can produce large number of on-shell J/ψ mesons at rest.

The experiment BESIII has clear advantages for the studies of production of such X particles in comparison with the experiments Belle II and BaBar where the continuum $e^+e^- \to \mu^+\mu^- X$ process can be considered [6]. First, at BESIII a very large number ($\sim 10^{11}$) of on-shell J/ψ particles (at rest) will be produced [7–9], and consequently the number of $J/\psi \to \mu^+\mu^- X$ events that can be produced is significantly higher than that at Belle II or BaBar. This is due to the fact that the continuum process $e^+e^- \to \mu^+\mu^- X$ at Belle II or BaBar does not take place via on-shell exchanged particle, making the number of such events considerably suppressed. Secondly, the center-of-mass energy $\sqrt{s}$ of the events at Belle II and BaBar is very high ($\approx 10\,\text{GeV}$), making the cross section of the considered process suppressed, $\sigma \propto 1/s$. In addition, since BESIII has the final state kinematics strongly constrained by the on-shell J/ψ (which has a very small decay width) without any initial soft photon radiation γ_{ISR}, the background effects are much easier to analyze than at Belle II or BaBar.

We would like to point out that our approach to study the bosonic mediators $X_{0,1}$ differs from another recent proposal [10], which studied J/ψ decay at BESIII through the process of $J/\psi \to X_{0,1} + \gamma \to \mu^-\mu^+\gamma$ in the range $m_{J/\psi} \geqslant m_X \geqslant 2m_\mu$: (1) Unlike our paper, ref. [10] does not consider the muon anomalous magnetic moment to probe and constrain the parameter space for $X_{0,1}$. (2) In ref. [10] the mediators $X_{0,1}$ can be scalar, pseudo-scalar, vector or axial-vector; while in our case, in order to explain the observed muon anomalous magnetic moment, we have constrained ourselves to the scalar and vector possibilities only, thus making the scenario much simpler. Probing such light scalar and vector particles have also been discussed in context of other decay modes in refs. [11–13] in context of specific U(1) extensions of the SM.

Our paper is organized as follows. In section 2 we elaborate on the two new physics scenarios under our consideration and clearly lay down the search strategy using the decay $J/\psi \to \mu^-\mu^+ X_{0,1}$. This is followed in section 3 by a numerical study of the two scenarios as well as that of the competing SM background processes, in context of the BESIII experiment. Finally we conclude in section 4 emphasizing the various salient features of our study.

2 Theoretical motivation and experimental search strategy

2.1 Simplest muonic interactions

For an effective solution to the problem of muon anomalous magnetic moment without affecting any other existing studies, it would be ideal if the new interactions that get introduced only involve muons. In this context it is well known that if there exists either a scalar X_0 or a vector X_1 that interacts only with the muons, we can write down the

JHEP10(2020)207

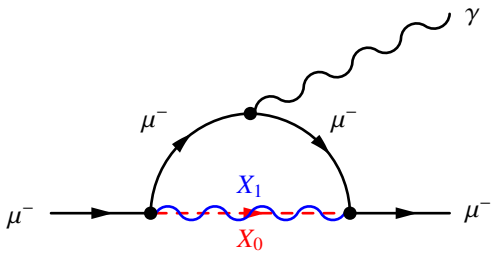

Figure 1. Contribution from X_0 or X_1 to muon anomalous magnetic moment.

following interaction Lagrangians:

$$\mathcal{L}_\mu^{\text{scalar}} = -g_0\, X_0\, \overline{\mu}\, \mu, \tag{2.1a}$$

$$\mathcal{L}_\mu^{\text{vector}} = -g_1\, X_{1\alpha}\, \overline{\mu}\, \gamma^\alpha\, \mu. \tag{2.1b}$$

These interactions give contributions to the muon anomalous magnetic moment. The leading order contributions, from the loops as shown in figure 1, are given by [14],

$$\Delta a_\mu^{\text{scalar}} = \frac{g_0^2}{8\pi^2} \int_0^1 dx\, \frac{m_\mu^2 (1-x)(1-x^2)}{m_\mu^2 (1-x)^2 + m_X^2 x}, \tag{2.2a}$$

$$\Delta a_\mu^{\text{vector}} = \frac{g_1^2}{8\pi^2} \int_0^1 dx\, \frac{2m_\mu^2\, x\, (1-x)^2}{m_\mu^2 (1-x)^2 + m_X^2 x}, \tag{2.2b}$$

where m_X is used to denote the mass of both X_0 and X_1 and these results are applicable for $m_X \lesssim 2m_\mu$. The region of parameter space in $g_{0,1}$-m_X planes allowed by the current discrepancy in anomalous magnetic moment (at 2σ level, adding the errors in eq. (1.1) by quadrature) is shown in figure 2. It must be noted that the condition $m_X < 2m_\mu$ is imposed to kinematically forbid the only possible tree-level decay $X_{0,1} \to \mu^-\mu^+$. Other decay modes, such as $X_{0,1} \to e^-e^+, \nu_\ell \overline{\nu}_\ell$ for $\ell = e, \mu, \tau$ are not allowed at the tree level, but in principle these are possible via loop processes which are suppressed if not forbidden kinematically.

It is important to note that we have considered in eq. (2.1) only parity even scenarios here, i.e. no pseudo-scalar or axial-vector possibilities are being considered. This is so because of the fact that the contribution of pseudo-scalar and axial-vector particles to the anomalous magnetic moment of muon has opposite sign which makes the discrepancy between theory prediction and experimental measurement much larger. Therefore, we shall limit ourselves to scalar and vector cases only. It is also interesting to note that the scalar and vector scenarios may have their origin in a more complete model. There are many UV complete models which can accommodate eqs. (2.1), but they have additional features which might constrain the model severely. In the next subsection we shall consider one of the simplest probable models elucidating the main ideas behind such an approach.

2.2 Towards a possibly complete model: $\mathrm{U}(1)_{L_\mu - L_\tau}$

Here we are concerned with a specific extension of the SM gauge group, namely by an additional symmetry group $\mathrm{U}(1)_{L_\mu - L_\tau}$ which conserves the difference between the muon and

JHEP10(2020)207

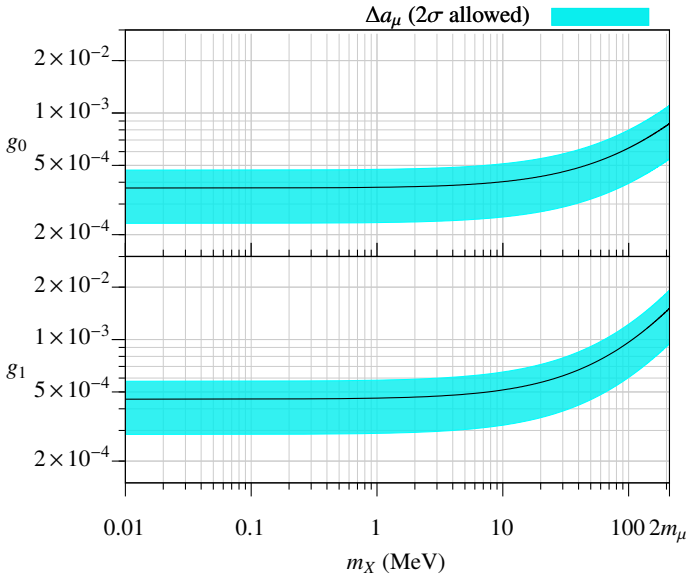

Figure 2. The parameters g_0, g_1 and $m_X \leqslant 2m_\mu$, as allowed by Δa_μ at 2σ level. Obtained by adding the errors in eq. (1.1) in quadrature and by using eq. (2.2). It is important to note here that $X_{0,1}$ are assumed to exclusively interact with muons alone as per eq. (2.1).

tau lepton numbers, while keeping the overall model anomaly free [15–17]. The new gauge symmetry, under which only the second and third generations of leptons are charged, gives rise to an additional massive vector gauge boson, X_1, which naturally couples to second and third generations of leptons alone at the tree level. The mass of the X_1 boson, m_X, can be generated via either spontaneous symmetry breaking or Stueckelberg mechanism [18, 19]. The underlying Lagrangian including the kinetic term, mass term and gauge interaction term, for the gauge boson X_1 is therefore given by,

$$\mathcal{L} \supset \mathcal{L}_{\rm SM} - \frac{1}{4} X_1^{\alpha\beta} X_{1\alpha\beta} + \frac{m_X^2}{2} X_1^\alpha X_{1\alpha} - X_{1\alpha} J^\alpha_{\mu-\tau}, \tag{2.3}$$

where $X_{1\alpha\beta} \equiv \partial_\alpha X_{1\beta} - \partial_\beta X_{1\alpha}$ is the field strength tensor, and $J^\alpha_{\mu-\tau}$ is the $\mu-\tau$ current given by,

$$J^\alpha_{\mu-\tau} = g_1 \left(\overline{\mu}\gamma^\alpha \mu - \overline{\tau}\gamma^\alpha \tau + \overline{\nu}_\mu \gamma^\alpha P_L \nu_\mu - \overline{\nu}_\tau \gamma^\alpha P_L \nu_\tau \right), \tag{2.4}$$

where $P_L \equiv \frac{1}{2}\left(1-\gamma^5\right)$ is the left projection operator. The first term in $J^\alpha_{\mu-\tau}$ in eq. (2.4) is same as the term in eq. (2.1b). However, in the $\mathrm{U}(1)_{L_\mu - L_\tau}$ extension of the Standard Model, there appear additional terms which would contribute to the anomalous magnetic moment of tau via a loop diagram similar to the one in figure 1. However, currently the anomalous magnetic moment of tau is not well measured to constrain these new physics scenarios [2]. Therefore, we shall refrain from using anomalous magnetic moment of tau in this paper. Nevertheless, in the $\mathrm{U}(1)_{L_\mu - L_\tau}$ extension, the X_1 vector boson is not necessarily stable even for $m_X < 2m_\mu$ as $X_1 \to \overline{\nu}_\mu \nu_\mu, \overline{\nu}_\tau \nu_\tau$ are allowed at the tree level. The decay $X_1 \to e^- e^+$ is still forbidden at the tree level and can only happen (if kinematically allowed) via quantum loop and it would therefore be suppressed. Thus, predominantly the X_1 boson would decay

JHEP10(2020)207

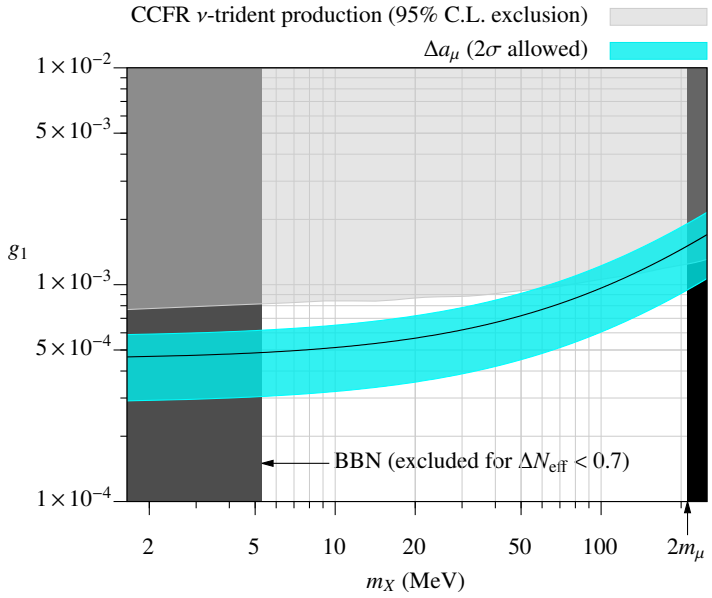

Figure 3. Allowed region in the g_1-m_X plane from anomalous magnetic moment of muon. Here we have combined the experimental and theoretical uncertainties in quadrature.

invisibly and its direct signature at experiments would be missing 4-momentum. Further, X_1 could also couple to dark matter constituting yet another invisible decay mode.

Considering only the $U(1)_{L_\mu - L_\tau}$ new physics and depending on whether the mass m_X is small or large, there exist other diverse observations which can also probe or constrain the allowed region in the g_1-m_X plane, such as (1) precision measurements at Z pole [6], (2) neutrino-nucleus scattering involved in neutrino trident production [20, 21], (3) rare kaon decays in beam-dump experiments [22], (4) tests of lepton universality such as $R(K)$, $R(K^*)$ [23–25] etc., as well as (5) big-bang nucleosynthesis with constraint on deviation from effective number of light neutrinos ($\Delta N_{\rm eff}$) [26–28]. In the mass range of our interest, i.e. $m_X < 2m_\mu$, the constraints from neutrino trident production as measured by the CCFR experiment [20] as well as the constraint from big-bang nucleosynthesis [26] are relevant and are shown in figure 3. It is very clear from figure 3 that the exclusion region from neutrino trident production experiment strongly constrains a portion of the parameter space allowed by muon anomalous magnetic moment in the higher mass ranges.

In order to probe the allowed parameter space in a more thorough manner, our chosen process must not only have high yield, but should have a distinct experimental signature in the parameter region of interest. In the next subsection, we analyze a decay mode which satisfies these criteria.

2.3 New search strategy

Since we are concerned with probing the scalar X_0 and vector boson X_1 (which can be called "muon-philic") as they satisfy the eq. (2.1), it is only natural to think of a process that involves muons in the final state to search for $X_{0,1}$. Moreover, as we have discussed above, $X_{0,1}$ with mass $m_X < 2m_\mu$ would be fully invisible as it is electrically neutral and

JHEP10(2020)207

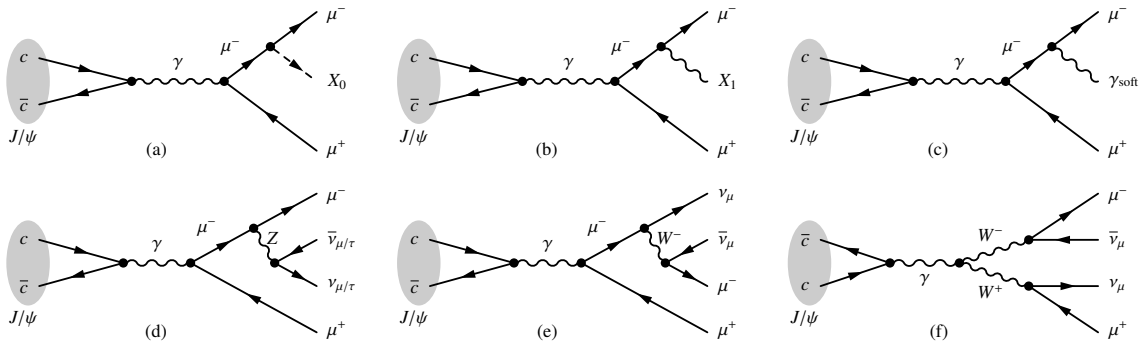

Figure 4. Quark-level diagrams for the new physics signal of X_0 or X_1 (a,b) and the dominant background from final state radiation of soft-photon (c) as well as the sub-dominant background processes (d,e,f) in the Standard Model. Diagrams (a), (b), (c), (d) and (e) have conjugate diagrams (with vertices on the μ^+ line) which are not drawn here. Charge conjugation invariance prevents radiation of soft photon from J/ψ.

stable (if it decays, then it decays to neutrino-antineutrino pair and possibly to dark matter particles, which are also invisible). Thus, the process we consider must have missing 4-momentum in the final state, and it should be possible, in principle and practice, to measure the missing 4-momentum as precisely as experimentally possible. An excellent process that satisfies all these criteria is the decay $J/\psi \to \mu^-\mu^+X_{0,1}$, where J/ψ needs to be produced at rest so that the initial 4-momentum is fully known and fixed. Because the final state has two muons which are well reconstructed in modern detectors, this would imply that the missing 4-momentum can be precisely inferred in such a case.

It is important to note that (1) extremely large sample of on-shell J/ψ can be produced in e^+e^- colliders such as BESIII, which provides statistically significant number of signal events, (2) the extremely narrow width of J/ψ ensures that events with the missing initial soft photon radiation $\gamma_{\rm ISR}$ from the colliding electron-positron beams can be safely ignored (unlike the continuum process of $e^-e^+ \to \mu^-\mu^+X_{0,1}$, where the initial state radiation of soft photons would be a major background) and (3) the missing final state soft photon radiation from the muons (as shown in figure 4(c)), which constitutes the dominant background for our decay $J/\psi \to \mu^-\mu^+X_{0,1}$, can also be dealt with very precisely due to the fact that $J/\psi \to \mu^-\mu^+$ is very well studied and the missing mass in $J/\psi \to \mu^-\mu^+\gamma_{\rm soft}$ events always peaks at the photon pole, i.e. at missing mass equal to zero. The continuum process $e^-e^+ \to \mu^-\mu^+X_{0,1}$, which can be studied at experiments such as Belle II has a much larger set of background processes and the strategy to be dealt with such a study can be found in ref. [6].

The quark-level Feynman diagrams for the signal and background processes are shown in figure 4. It should be noted that, except the final state soft radiation (shown in figure 4(c)), the other backgrounds (shown in figure 4(d,e,f)) are extremely suppressed as they involve two or more weak vertices. Quantitatively, the soft photon background dominates over the weak background by roughly eight orders of magnitude. Therefore, we shall not dwell upon any of the weak background processes, shown in figure 4, in our numerical studies.

JHEP10(2020)207

Now, considering the signal events alone in the context of the BESIII experiment where it is estimated that 10^{11} number of J/ψ would be produced, we find that roughly 300–2000 events of $J/\psi \to \mu^-\mu^+X_1$ or about 30–300 events of $J/\psi \to \mu^-\mu^+X_0$ can be expected (see figure 5), corresponding to the region of parameter space allowed by the muon anomalous magnetic moment. Due to this large number of events expected, if we observe fewer or no events, then this would rule out the simplistic scalar and vector explanation of muon anomalous magnetic moment which we considered here. In order to fully understand the feasibility of the decay $J/\psi \to \mu^-\mu^+X_{0,1}$, we made a comparative study of the dominant SM background and the new physics events in the following section.

3 Numerical study of feasibility of probing the new physics scenarios

As we have mentioned in the previous section, the final state radiation of soft photon from either of the muon lines is the dominant as well as the only relevant background in our case. We have devised a non-traditional approach to study the dominant background process $J/\psi \to \mu^-\mu^+\gamma_{\rm soft}$. Since the soft photon is not detected, the observed events are essentially $J/\psi \to \mu^-\mu^+$ events as the soft-photon has low energy (BESIII cannot detect soft photons with energy $< 20\,\text{MeV}$ [36]) and hence it also has a small magnitude of 3-momentum, essentially keeping the two final muons back-to-back, within the accuracy of the experimental resolution of the muon tracks (provided J/ψ is produced at rest, which is true for the BESIII experiment). Therefore, if we take the muon momentum resolution of the experiment into account for the muon pair in $J/\psi \to \mu^-\mu^+$, we can essentially get all possible soft-photon events as required for our numerical study. At BESIII the error in the momentum resolution is about 1% of the momentum being measured [36], i.e. the experimental uncertainty in the measurement $\sigma_p \sim 0.01p$ where p is the central value of the magnitude of the 4-momentum. For simplicity, we have specifically assumed $\sigma_p \sim 15\,\text{MeV}$ for our numerical simulation, which would presumably provide bigger momentum uncertainty for most events than what is expected experimentally. We utilize a multitude of observables and relevant cuts, as discussed below, to distinguish the signal and background events so as to facilitate the discovery of new physics in our decay mode $J/\psi \to \mu^-\mu^+X_{0,1}$. For our numerical study we have considered 10^{11} number of J/ψ that would be produced at rest at the BESIII experiment. In the numerical simulation of signal events we have also considered the central value of $g_{0,1}$ for the corresponding value of m_X as allowed by the muon anomalous magnetic moment, see figure 5. Below we first illustrate our methodology for the vector boson case and finally discuss the scalar case and compare.

3.1 Probing the vector boson case

3.1.1 Square of the missing mass

If we denote the 4-momenta of J/ψ, μ^-, μ^+ and the missing component (which can be the new particles $X_{0,1}$ or soft photon $\gamma_{\rm soft}$) by p_J, p_-, p_+ and $p_{\rm miss}$, then the missing mass $m_{\rm miss}$ is given by,

$$m^2_{\rm miss} \equiv p^2_{\rm miss} = (p_J - p_- - p_+)^2 \,. \tag{3.1}$$

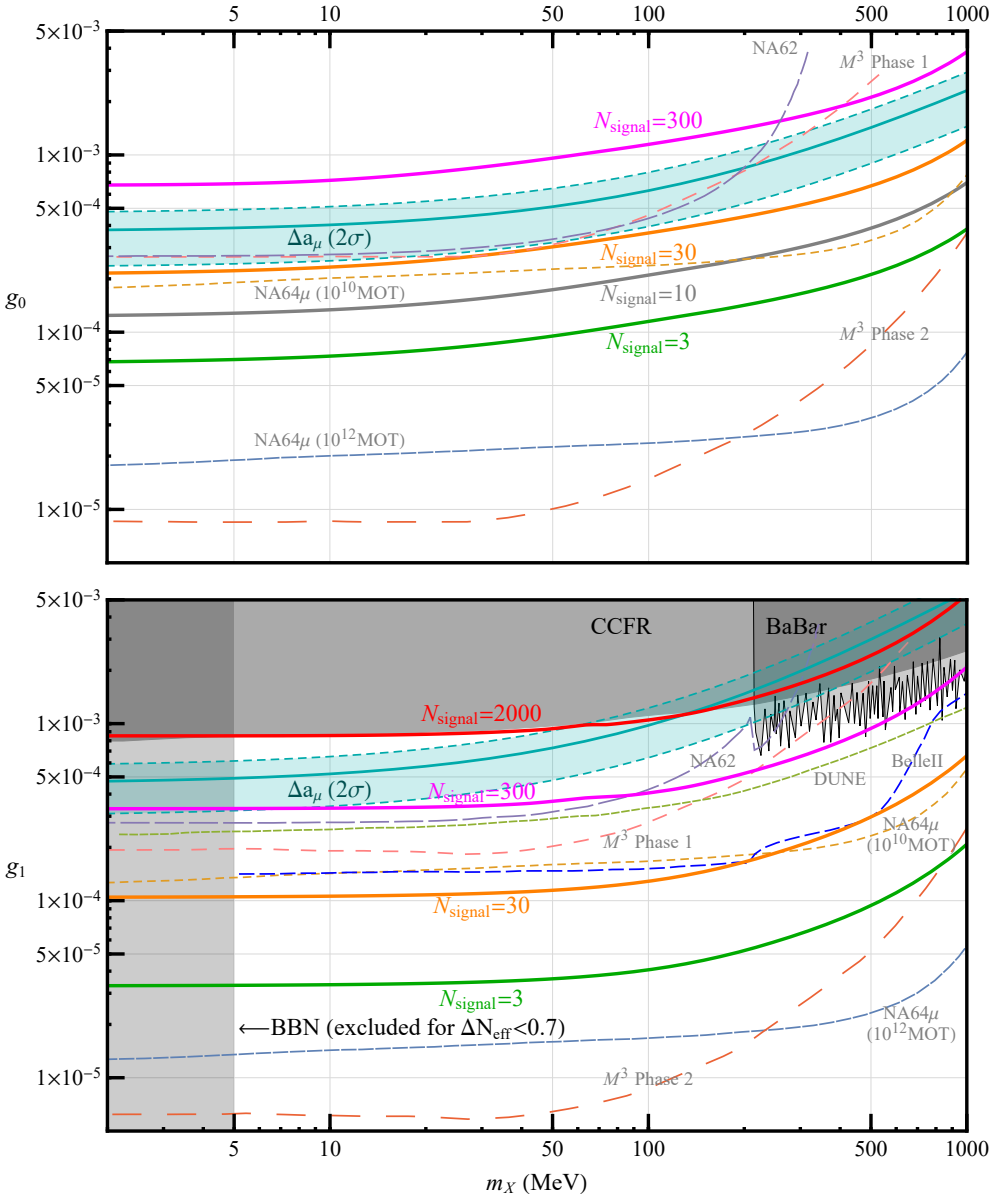

Figure 5. Estimate of number of $J/\psi \to \mu^-\mu^+X_{0,1}$ events in the $g_{0,1}$-m_X parameter space in context of BESIII experiment. The parameter space allowed by Δa_μ at 2σ level would give rise to about 300–2000 signal events for $J/\psi \to \mu^-\mu^+X_1$ decay, and 30–300 signal events for $J/\psi \to \mu^-\mu^+X_0$ decay at the BESIII experiment. These numbers are obtained after considering an energy cut, which will be discussed in section 3.1.2. For a direct comparison we have also included sensitivity limits achievable from other future experiments, such as muon scattering off nuclei in M^3 [29] (pink dashed line for M^3 phase 1 and dark orange dashed line for M3 phase 2) and NA64μ [30–33] (golden dashed line for NA64μ with 10^{10} muons on target and sky blue dashed line for NA64μ with 10^{12} muons on target), rare kaon decay in NA62 [34] (violet dashed line), neutrino tirdent experiment at DUNE [35] (olive dashed line) and the continuum $e^+e^- \to \mu^+\mu^-X$ process at Belle II [6] (blue dashed line).

JHEP10(2020)207

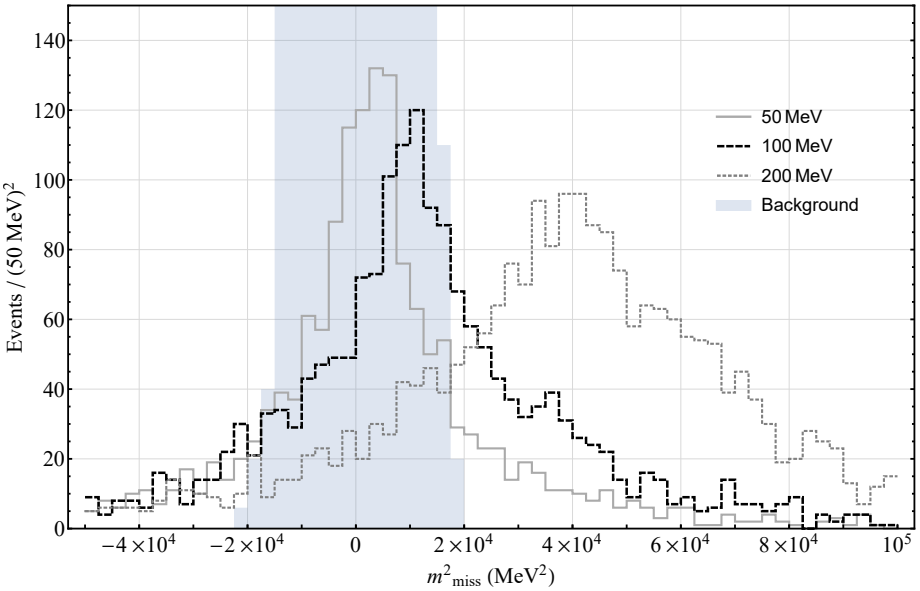

Figure 6. Distribution of missing mass square for both signal events $J/\psi \to \mu^-\mu^+ X_1$ and background events $J/\psi \to \mu^-\mu^+\gamma_{\rm soft}$. (Here the background is composed of not only $J/\psi \to \mu^-\mu^+\gamma_{\rm soft}$ but also experimentally smeared $J/\psi \to \mu^-\mu^+$.) The central value of g_1 that solves Δa_μ for the corresponding value of m_X (central value of figure 2) is used for the demonstration. Shifts in g_1 will only scale the distribution accordingly. The bin size of 50 MeV for missing mass does not imply that mass of X_1 can not be probed below 50 MeV.

Theoretically $m^2_{\rm miss}$ distribution for signal events will be characterized by very sharp peaks due to the tiny decay width of $X_{0,1}$, e.g. in the $\mathrm{U}(1)_{L_\mu - L_\tau}$ model the $X_1 \to \nu_\mu\overline{\nu}_\mu, \nu_\tau\overline{\nu}_\tau$ decays provide $\Gamma_{X_1} = g_1^2\, m_X/(12\pi)$, and the background events should be crowded at $m^2_{\rm miss} = 0$. However errors in measurements of momenta will smear the distribution of events for both signal and background.

The results from our simulation for both signal and background events are shown in figure 6. We have shown $m^2_{\rm miss}$ distribution for three different signal cases corresponding to $m_X = 50\,\mathrm{MeV}$, 100 MeV and 200 MeV. It is easy to observe a corresponding shift in the position of the signal peaks when we go from smaller mass to the larger mass. The background is large in the neighborhood of $m^2_{\rm miss} = 0$, as expected. It can be seen from figure 6 that the background events dominate up to around $m^2_{\rm miss} \sim (120\,\mathrm{MeV})^2$. This especially kills signal events with $m^2_{\rm miss} < (120\,\mathrm{MeV})^2$ and makes it difficult to accurately identify m_X, the mass of X_1. In order to identify m_X, we need to use the missing energy information and apply energy cut as discussed below.

3.1.2 Missing energy

The missing energy $E_{\rm miss}$ is defined as

$$E_{\rm miss} \equiv M_{J/\psi} - E_+ - E_-, \tag{3.2}$$

where $M_{J/\psi}$ is the mass of J/ψ, $E_\pm$ denote the energies of $\mu^\pm$. The $E_{\rm miss}$ distribution of a simulated background as well as few benchmark signal cases (corresponding to $m_X =$

JHEP10(2020)207

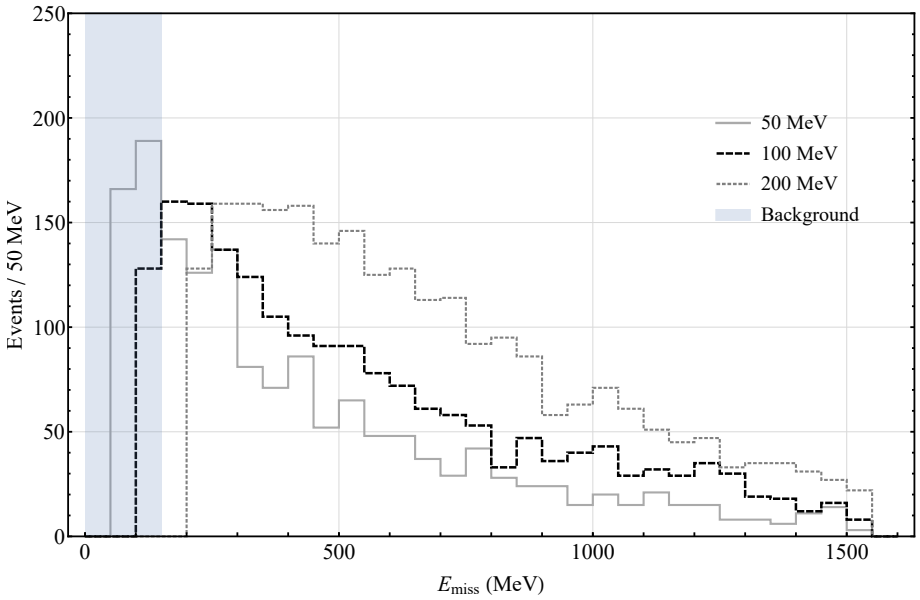

Figure 7. Distribution of missing energy for the signal events $J/\psi \to \mu^-\mu^+ X_1$ and the background events $J/\psi \to \mu^-\mu^+\gamma_{\text{soft}}$. Here the bin size for missing energy is 50 MeV. All the background events are confined to the region $E_{\text{miss}} < 140\,\text{MeV}$. Thus for signal events with $m_X \lesssim 50\,\text{MeV}$ the missing energy peaks cannot be observed after imposing the $E_{\text{miss}} < 140\,\text{MeV}$ cut.

m_X[MeV]	$\overline{\text{Br}}$	N_{signal}	$N^{\text{cut}}_{\text{signal}}$
50	0.032505	1546	1236
100	0.022285	1840	1747
150	0.016889	2127	2127
200	0.010947	2378	2378

Table 1. Canonical branching fractions and the number of signal events before and after applying the missing energy cut, $E_{\text{miss}} = 140\,\text{MeV}$. The central value of g_1 that solves Δa_μ for the corresponding value of m_X (central value of figure 2) is used for computing the number of signal events.

50 MeV, 100 MeV and 200 MeV) are shown in figure 7. The figure shows that the energy cut around 140 MeV will completely eliminate the background events (as the missing soft-photon would have energy $< 20\,\text{MeV}$ at BESIII), while leaving most of signal events.

In table 1 we list the canonical branching ratio, $\overline{\text{Br}} \equiv \text{Br}/g_1^2$, and the number of signal events before and after applying the missing energy cut by which we throw away all those events with $E_{\text{miss}} < 140\,\text{MeV}$. Only the number of signal events with lighter m_X (around 50 MeV) is significantly reduced. After applying the missing energy cut the m^2_{miss} distributions gets modified as is shown in figure 8. The figure shows clearly that no background events survive after this cut is imposed. Now the new gauge boson mass can be extracted from the resultant distribution, shown in figure 8. Please note that although the demonstrations were made with the specific values of g_1, which solve the muon anomalous magnetic moment for corresponding m_X, the strategy is generic and changes in g_1 will end

JHEP10(2020)207

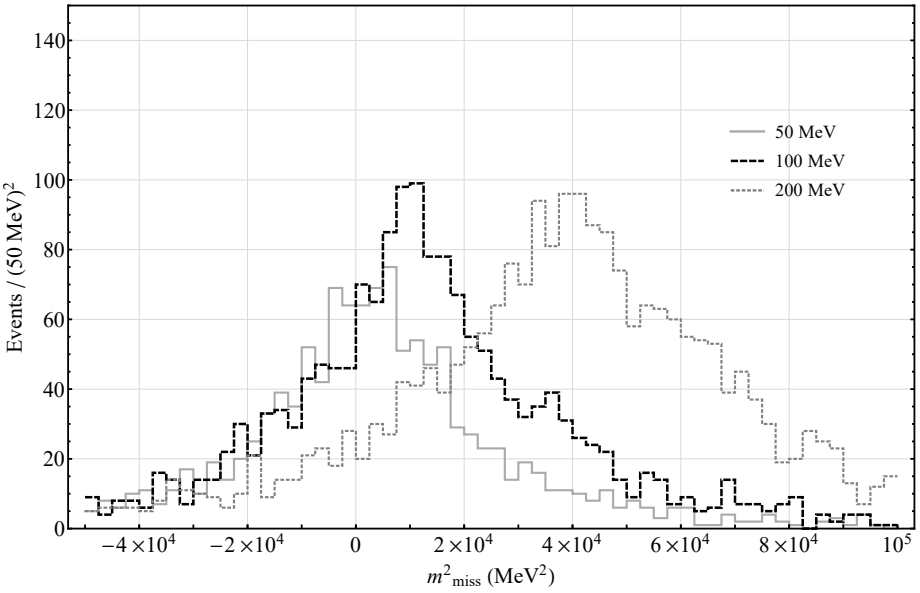

Figure 8. Distribution of missing mass square after applying the minimum missing energy cut of 140 MeV.

up with nothing more than overall scaling of the number of events (in figures 6, 7, 8, 9 and table 1), while leaving the overall shapes of distributions unchanged.

3.1.3 Mass shift of muon pair from J/ψ

Alternatively one can utilize another observable to probe X_1, namely the deviation in the measurement of invariant mass of observed muon pair from mass of J/ψ,

$$\Delta(M_{J/\psi}) \equiv M_{J/\psi} - \sqrt{(p_+ + p_-)^2}. \tag{3.3}$$

If this value significantly deviates from zero for a distribution of events, those events would qualify as signal events. In the case of background event $J/\psi \to \mu^-\mu^+\gamma_{\rm soft}$, $\Delta(M_{J/\psi})$ indicates difference between the actual and observed mass of J/ψ. So it will be peaked at zero with some smearing due to error in momentum measurement. Taking the energy and momentum resolution at BESIII experiment, the standard deviation of $\Delta(M_{J/\psi})$ distribution comes around 11 MeV and so there will be some events up to around 70 MeV. This is shown in the figure 9.

It is easy to show that

$$\Delta(M_{J/\psi}) \simeq M_{J/\psi} - \sqrt{M_{J/\psi}^2 + m_X^2 - 2M_{J/\psi}\, E_X}, \tag{3.4}$$

where E_X is the energy of X_1 and it is the same as $E_{\rm miss}$, the latter was analyzed in section 3.1.2 and figure 7 for a few benchmark signal scenarios. The minimum value of measured $\Delta(M_{J/\psi})$ is equal to m_X when we substitute the minimum value of $E_X = m_X$ in eq. (3.4). Thus the mass of X_1 can, in principle, be inferred from figure 9 by reading the minimum value of $\Delta\left(M_{J/\psi}\right)$ for the corresponding distribution. However, this information is also subject to the smearing effect from momentum resolution. Nevertheless, looking at

JHEP10(2020)207

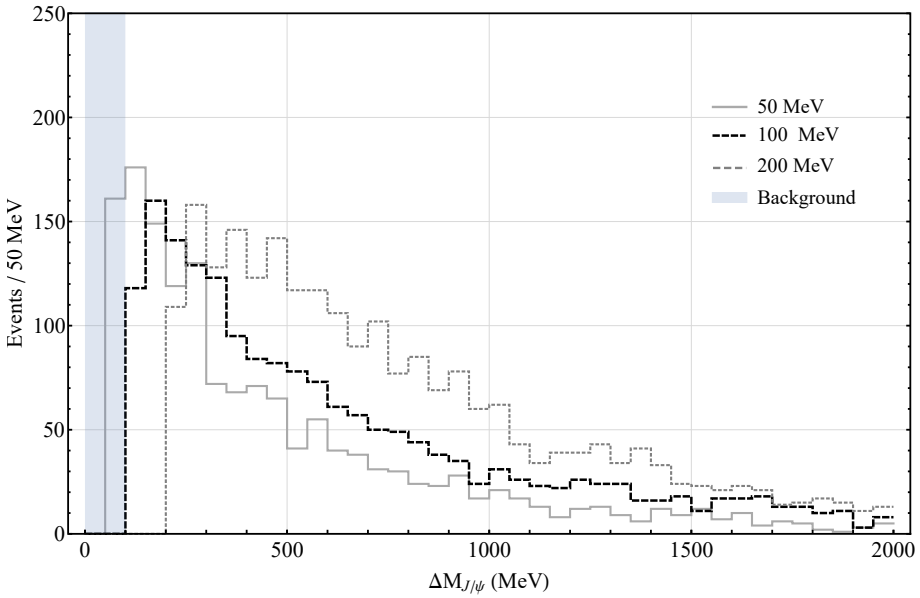

Figure 9. Distribution of the mass shift $\Delta(M_{J/\psi})$ for the signal events $J/\psi \to \mu^-\mu^+ X_1$ and the background events $J/\psi \to \mu^-\mu^+\gamma_{\text{soft}}$. The effect of background is negligible here, considering the long tail of the $\Delta(M_{J/\psi})$ distribution of the signal. The background goes up to around 70 MeV and it can be clearly distinguished from the signal for heavier X_1 cases.

m_X[MeV]	$\overline{\text{Br}}_{\text{scalar}}$	$\overline{\text{Br}}_{\text{vector}}$
50	0.0033254	0.032505
100	0.0022872	0.022285
150	0.0017978	0.016889
200	0.0014913	0.010947

Table 2. Comparison of canonical branching ratios of $J/\psi \to \mu^-\mu^+ X_{0,1}$ for a few chosen values of m_X.

the $\Delta(M_{J/\psi})$ distribution would complement our search for new physics using previously discussed observables. An important feature of the $\Delta(M_{J/\psi})$ distribution is that it runs up to much larger values for a signal compared to the background, even after smearing is taken into account. Especially, if the mass of X_1 is larger than 70 MeV, the signal can be easily distinguished from the background.

3.2 Probing the scalar case

Comparing the canonical branching ratios of the scalar and vector cases, we find that in the scalar case they are about 10 times smaller than in the vector case, see table 2. Nevertheless, applying the same techniques as discussed above for the vector case, we can also probe the scalar new physics possibility. It is important to note that the missing energy distribution of a scalar is different from that of a vector case. In figure 10 we plotted the canonical differential decay rates $d\overline{\Gamma}_{0,1}/dE_{\text{miss}}$ (where $\overline{\Gamma}_{0,1} \equiv \Gamma/g^2_{0,1}$ is the canonical decay width) for the scalar and vector cases, respectively. It is clear that scalar new physics prefers higher

JHEP10(2020)207

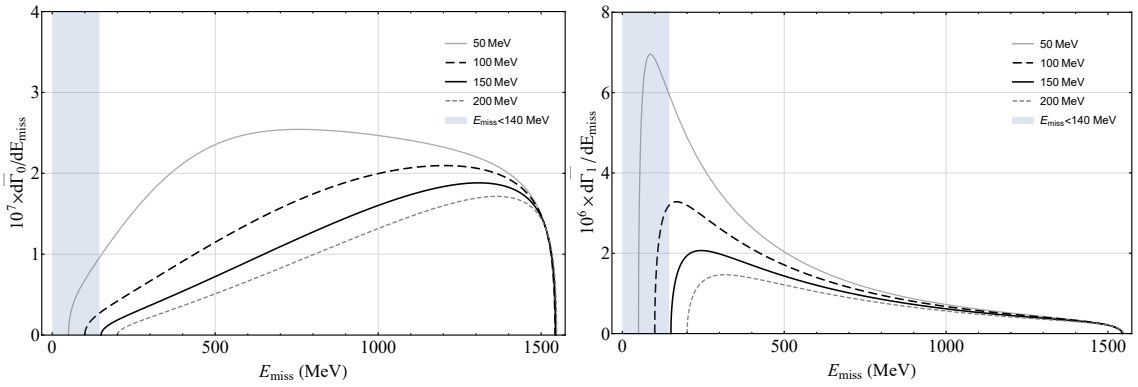

Figure 10. The unnormalized canonical missing energy distributions for scalar $d\overline{\Gamma}_0/dE_{\rm miss}$ and vector $d\overline{\Gamma}_1/dE_{\rm miss}$ new physics cases with different values of m_X. The scalar cases exhibit a preference for higher missing energy as opposed to the vector cases.

missing energy whereas vector new physics prefers lower missing energy. Thus, one can easily distinguish them in an experiment once either of them gets detected.

4 Conclusion

We investigated the possible $J/\psi \to \mu^+\mu^- X$ events at the BESIII experiment, where X is a vector (or scalar) "muon-philic" particle which could explain the present discrepancy $\Delta a_\mu \equiv a_\mu^{\rm exp} - a_\mu^{\rm SM}$ of the anomalous magnetic moment of μ lepton, cf. eq. (1.1). It turns out that, if the coupling of X to muon is $g_{0,1} \sim 4 \times 10^{-4}$–$10^{-3}$ and its mass is $m_X < 2m_\mu$, this particle can explain the mentioned discrepancy Δa_μ.

The advantage of BESIII, in comparison with other experiments (Belle II and BaBar) where the continuum process $e^+e^- \to \mu^+\mu^- X$ is considered, is that at BESIII there will be produced a very large number ($\sim 10^{11}$) of on-shell J/ψ particles (at rest) without any initial soft photon radiation. Thus, the number of $J/\psi \to \mu^+\mu^- X$ events can be significantly higher than at Belle II or BaBar, because the latter experiments do not have on-shell intermediaries for the continuum process $e^+e^- \to \mu^+\mu^- X$. Further, the final state kinematics is more constrained at BESIII because of the mentioned on-shellness and the very small decay width of J/ψ, making the background effects smaller and easier to analyze than at Belle II or BaBar. In addition, the center-of-mass energy at Belle II and BaBar is very high, which makes the cross sections of $e^+e^- \to \mu^+\mu^- X$ suppressed ($\sigma \propto 1/s$).

In figure 5 we have provided a comparison of the sensitivity limits on the parameter space $(g_{0,1}, m_X)$ from our approach to those achievable by other future experiments. It clearly shows the competitiveness of our search method for both scalar and vector new physics. We showed that the number of events $J/\psi \to \mu^+\mu^- X$ that take place at BESIII in the mentioned range of parameters $(g_{0,1}, m_X)$ is $\sim 10^3$ when X is vector, and $\sim 10^2$ when X is scalar. The main background to these events at BESIII is the final state radiation $J/\psi \to \mu^+\mu^-\gamma$. This is in contrast with Belle II [6] (and BaBar) background to $e^+e^- \to \mu^+\mu^- X$, where initial state radiation and $e^+e^- \to \tau^+\tau^- \to \mu^+\nu_\mu\bar{\nu}_\tau\mu^-\bar{\nu}_\mu\nu_\tau$ are additional background sources. We showed that the distribution $m^2_{\rm miss}$, eq. (3.1), is

JHEP10(2020)207

a priori not a good quantity to identify the signal events $J/\psi \to \mu^+\mu^- X$, because of strong background ($J/\psi \to \mu^+\mu^-\gamma$) contributions to this quantity. On the other hand, the distribution $dN_{J/\psi\to\mu\mu X}/dE_{\rm miss}$, where $E_{\rm miss} = M_{J/\psi} - E_+ - E_-$ [cf. eq. (3.2)], is a good quantity to identify the signal events when $m_X > 50\,\text{MeV}$ (and $m_X < 2m_\mu$) once the cut $E_{\rm miss} < 140\,\text{MeV}$ is applied which eliminates the background; for $m_X < 50\,\text{MeV}$, the signal rate gets significantly diminished by the cut and the maximum is swamped by the background. The mentioned cut $E_{\rm miss} < 140\,\text{MeV}$ also eliminates completely the background to the quantity $m^2_{\rm miss}$. Further, we showed that the quantity $\Delta(M_{J/\psi})$, defined in eq. (3.3), is a good complementary quantity to identify the signal events if $m_X > 70\,\text{MeV}$. If X is a scalar, the number of events in the mentioned parameter range of $(g_{0,1}, m_X)$ is by about a factor of 10 lower, as mentioned earlier. However, the form of the distribution $dN_{J/\psi\to\mu\mu X}/dE_{\rm miss}$ is in this case shifted to higher values of $E_{\rm miss}$, allowing the scalar case to be easily distinguished from the vector case.

In summary, in this paper we demonstrated that it is possible to not only probe both the scalar and vector new physics cases contributing to anomalous magnetic moment of muon by searching for the signal $J/\psi \to \mu^-\mu^+ +$ "missing," but also to distinguish between the SM background and the new physics possibilities by using missing mass, missing energy and mass shift of muon pair from J/ψ. Our numerical analysis clearly shows that BESIII could be the best place, at present, to implement this study experimentally. The amazing aspect of this probe is the possibility to either discover new physics or to completely rule out the simplest explanations for the longstanding muon anomalous magnetic moment discrepancy.

Acknowledgments

The work of C.S.K., D.H.L. and D.S. was supported by the National Research Foundation of Korea (NRF) grant funded by the Korean government (MSIP) (NRF2018R1A4A1025334); the work of G.C. was supported by FONDECYT (Chile) Grant No. 1180344.

References

[1] Muon g-2 collaboration, *Final Report of the Muon E821 Anomalous Magnetic Moment Measurement at BNL*, *Phys. Rev. D* **73** (2006) 072003 [hep-ex/0602035] [INSPIRE].

[2] Particle Data Group collaboration, *Review of Particle Physics*, *Phys. Rev. D* **98** (2018) 030001 [INSPIRE].

[3] F. Campanario et al., *Standard model radiative corrections in the pion form factor measurements do not explain the a_μ anomaly*, *Phys. Rev. D* **100** (2019) 076004 [arXiv:1903.10197] [INSPIRE].

[4] F. Jegerlehner, *Muon $g-2$ theory: The hadronic part*, *EPJ Web Conf.* **166** (2018) 00022 [arXiv:1705.00263] [INSPIRE].

JHEP10(2020)207

[5] M. Davier, A. Hoecker, B. Malaescu and Z. Zhang, *A new evaluation of the hadronic vacuum polarisation contributions to the muon anomalous magnetic moment and to $\alpha(m_Z^2)$*, *Eur. Phys. J. C* **80** (2020) 241 [*Erratum ibid.* **80** (2020) 410] [arXiv:1908.00921] [INSPIRE].

[6] Y. Jho, Y. Kwon, S.C. Park and P.-Y. Tseng, *Search for muon-philic new light gauge boson at Belle II*, *JHEP* **10** (2019) 168 [arXiv:1904.13053] [INSPIRE].

[7] BESIII collaboration, *A sample of 10 billion J/ψ events together with a continuum data sample*, http://bes3.ihep.ac.cn/doc/3313.html, 11 February 2019.

[8] C.-Z. Yuan and S.L. Olsen, *The BESIII physics programme*, *Nature Rev. Phys.* **1** (2019) 480 [arXiv:2001.01164] [INSPIRE].

[9] BESIII collaboration, *Future Physics Programme of BESIII*, *Chin. Phys. C* **44** (2020) 040001 [arXiv:1912.05983] [INSPIRE].

[10] J. Jiang, H. Yang and C.-F. Qiao, *Exploring Bosonic Mediator of Interaction at BESIII*, *Eur. Phys. J. C* **79** (2019) 404 [arXiv:1810.05790] [INSPIRE].

[11] F.C. Correia and S. Fajfer, *Restrained dark $\mathrm{U}(1)_d$ at low energies*, *Phys. Rev. D* **94** (2016) 115023 [arXiv:1609.00860] [INSPIRE].

[12] F.C. Correia and S. Fajfer, *Light mediators in anomaly free $\mathrm{U}(1)_X$ models. Part I. Theoretical framework*, *JHEP* **10** (2019) 278 [arXiv:1905.03867] [INSPIRE].

[13] F.C. Correia and S. Fajfer, *Light mediators in anomaly free $\mathrm{U}(1)_X$ models. Part II. Constraints on dark gauge bosons*, *JHEP* **10** (2019) 279 [arXiv:1905.03872] [INSPIRE].

[14] M. Lindner, M. Platscher and F.S. Queiroz, *A Call for New Physics: The Muon Anomalous Magnetic Moment and Lepton Flavor Violation*, *Phys. Rept.* **731** (2018) 1 [arXiv:1610.06587] [INSPIRE].

[15] X. He, G.C. Joshi, H. Lew and R. Volkas, *New Z' phenomenology*, *Phys. Rev. D* **43** (1991) R22.

[16] X.-G. He, G.C. Joshi, H. Lew and R.R. Volkas, *Simplest Z' model*, *Phys. Rev. D* **44** (1991) 2118 [INSPIRE].

[17] R. Foot, X.G. He, H. Lew and R.R. Volkas, *Model for a light Z' boson*, *Phys. Rev. D* **50** (1994) 4571 [hep-ph/9401250] [INSPIRE].

[18] H. Ruegg and M. Ruiz-Altaba, *The Stueckelberg field*, *Int. J. Mod. Phys. A* **19** (2004) 3265 [hep-th/0304245] [INSPIRE].

[19] D. Feldman, Z. Liu and P. Nath, *The Stueckelberg Z Prime at the LHC: Discovery Potential, Signature Spaces and Model Discrimination*, *JHEP* **11** (2006) 007 [hep-ph/0606294] [INSPIRE].

[20] CCFR collaboration, *Neutrino tridents and W-Z interference*, *Phys. Rev. Lett.* **66** (1991) 3117 [INSPIRE].

[21] W. Altmannshofer, S. Gori, M. Pospelov and I. Yavin, *Neutrino Trident Production: A Powerful Probe of New Physics with Neutrino Beams*, *Phys. Rev. Lett.* **113** (2014) 091801 [arXiv:1406.2332] [INSPIRE].

[22] G. Krnjaic, G. Marques-Tavares, D. Redigolo and K. Tobioka, *Probing Muonphilic Force Carriers and Dark Matter at Kaon Factories*, *Phys. Rev. Lett.* **124** (2020) 041802 [arXiv:1902.07715] [INSPIRE].

JHEP10(2020)207

[23] R. Gauld, F. Goertz and U. Haisch, *An explicit Z'-boson explanation of the $B \to K^* \mu^+ \mu^-$ anomaly*, *JHEP* **01** (2014) 069 [arXiv:1310.1082] [INSPIRE].

[24] G. D'Amico et al., *Flavour anomalies after the R_{K^*} measurement*, *JHEP* **09** (2017) 010 [arXiv:1704.05438] [INSPIRE].

[25] G. D'Ambrosio, A.M. Iyer, F. Piccinini and A.D. Polosa, *Confronting B anomalies with low energy parity violation*, *Phys. Rev. D* **101** (2020) 035025 [arXiv:1902.00893] [INSPIRE].

[26] A. Kamada and H.-B. Yu, *Coherent Propagation of PeV Neutrinos and the Dip in the Neutrino Spectrum at IceCube*, *Phys. Rev. D* **92** (2015) 113004 [arXiv:1504.00711] [INSPIRE].

[27] M. Escudero, D. Hooper, G. Krnjaic and M. Pierre, *Cosmology with a very light $L_\mu - L_\tau$ gauge boson*, *JHEP* **03** (2019) 071 [arXiv:1901.02010] [INSPIRE].

[28] A. Kamada, K. Kaneta, K. Yanagi and H.-B. Yu, *Self-interacting dark matter and muon $g-2$ in a gauged $\mathrm{U}(1)_{L_\mu - L_\tau}$ model*, *JHEP* **06** (2018) 117 [arXiv:1805.00651] [INSPIRE].

[29] Y. Kahn, G. Krnjaic, N. Tran and A. Whitbeck, *M^3: a new muon missing momentum experiment to probe $(g-2)_\mu$ and dark matter at Fermilab*, *JHEP* **09** (2018) 153 [arXiv:1804.03144] [INSPIRE].

[30] S.N. Gninenko, N.V. Krasnikov and V.A. Matveev, *Muon $g-2$ and searches for a new leptophobic sub-GeV dark boson in a missing-energy experiment at CERN*, *Phys. Rev. D* **91** (2015) 095015 [arXiv:1412.1400] [INSPIRE].

[31] NA64 Collaboration, *Prospects for exploring the Dark Sector physics and rare processes with NA64 at the CERN SPS*, https://indico.cern.ch/event/765096/contributions/3295517/.

[32] NA64 collaboration, *Addendum to the Proposal P348: Search for dark sector particles weakly coupled to muon with NA64μ*, CERN-SPSC-2018-024, SPSC-P-348-ADD-3 (2018).

[33] J. Beacham et al., *Physics Beyond Colliders at CERN: Beyond the Standard Model Working Group Report*, *J. Phys. G* **47** (2020) 010501 [arXiv:1901.09966] [INSPIRE].

[34] G. Krnjaic, G. Marques-Tavares, D. Redigolo and K. Tobioka, *Probing Muonphilic Force Carriers and Dark Matter at Kaon Factories*, *Phys. Rev. Lett.* **124** (2020) 041802 [arXiv:1902.07715] [INSPIRE].

[35] P. Ballett, M. Hostert, S. Pascoli, Y.F. Perez-Gonzalez, Z. Tabrizi and R. Zukanovich Funchal, *$Z's$ in neutrino scattering at DUNE*, *Phys. Rev. D* **100** (2019) 055012 [arXiv:1902.08579] [INSPIRE].

[36] BESIII collaboration, *Design and Construction of the BESIII Detector*, *Nucl. Instrum. Meth. A* **614** (2010) 345 [arXiv:0911.4960] [INSPIRE].

JHEP10(2020)207